Scientific Reports

https://doi.org/10.1038/s41598-026-44173-5

Article in Press

GPER agonist G1 suppresses neuronal apoptosis mediated by endoplasmic reticulum stress after exertional heat stroke injury

Received: 13 November 2025

Accepted: 10 March 2026

Published online: 11 March 2026

Cite this article as: Han Z., Wang X., Guo J. *et al.* GPER agonist G1 suppresses neuronal apoptosis mediated by endoplasmic reticulum stress after exertional heat stroke injury. *Sci Rep* (2026). https://doi.org/10.1038/s41598-026-44173-5

Ziwei Han, Xiaochen Wang, Jiansong Guo, Chao Liu, Yan Shen, Baisheng Sun, Jie Hu, Zhi Mao & Feihu Zhou

We are providing an unedited version of this manuscript to give early access to its findings. Before final publication, the manuscript will undergo further editing. Please note there may be errors present which affect the content, and all legal disclaimers apply.

If this paper is publishing under a Transparent Peer Review model then Peer Review reports will publish with the final article.

ARTICLE IN PRESS

© The Author(s) 2026. **Open Access** This article is licensed under a Creative Commons Attribution-NonCommercial-NoDerivatives 4.0 International License, which permits any non-commercial use, sharing, distribution and reproduction in any medium or format, as long as you give appropriate credit to the original author(s) and the source, provide a link to the Creative Commons licence, and indicate if you modified the licensed material. You do not have permission under this licence to share adapted material derived from this article or parts of it. The images or other third party material in this article are included in the article's Creative Commons licence, unless indicated otherwise in a credit line to the material. If material is not included in the article's Creative Commons licence and your intended use is not permitted by statutory regulation or exceeds the permitted use, you will need to obtain permission directly from the copyright holder. To view a copy of this licence, visit http://creativecommons.org/licenses/by-nc-nd/4.0/.

GPER agonist G1 suppresses neuronal apoptosis mediated by endoplasmic reticulum stress after exertional heat stroke injury

Ziwei Han[1,2,5*], Xiaochen Wang [2,3,4*], Jiansong Guo[5], Chao Liu[1,2], Yan Shen[1], Baisheng Sun[1,2], Jie Hu[2], Zhi Mao[2], Feihu Zhou[1,2,4#]

[1]Medical School of Chinese PLA, Beijing, People's Republic of China

[2]Department of Critical Care Medicine, First Medical Center of Chinese PLA General Hospital, Beijing, People's Republic of China

[3]School of Medicine, Nankai University, Tianjin, People's Republic of China

[4]Department of Nephrology, First Medical Center of Chinese PLA General Hospital, State Key Laboratory of Kidney Diseases, National Clinical Research Center for Kidney Diseases, Beijing Key Laboratory of Kidney Diseases Research, Beijing, People's Republic of China

[5] Department of Critical Care Medicine, Chinese PLA 951 Hospital, Xinjiang Korla, 841000, China

* These authors contributed equally to this work.

#Correspondence to: Feihu Zhou

E-mail: feihuzhou301@126.com

Phone: 18699320551

ORCID: 0000-0002-1308-4034

Abstract

Exertional heat stroke (EHS) poses a significant public health challenge because of its elevated rates of mortality and disability. Sex differences in incidence have been noted, and estrogen may be a contributing factor. The innovative G protein-coupled estrogen receptor (GPER) is recognized for its protective function in various diseases via the rapid non-genomic pathway associated with estrogen. The neuroprotective effects of the GPER agonist G1 are well known, but its potential to improve EHS-related brain injury has not been explored. We investigated whether G1 can improve EHS-related brain injury and clarified the mechanisms underlying its protective effects. Twenty-four hours after injury, transcriptome sequencing was conducted, disclosing varying gene expression patterns within the mouse hippocampus. Increased expression of stress-related genes within the endoplasmic reticulum (ER) of EHS mice was noted. The activation of GPER through G1 led to reduction in the levels of ER stress-related proteins, including CHOP, GRP78, and caspase-12. This, in turn, diminished neuronal apoptosis caused by ER stress and enhanced both the survival rate and cognitive abilities of EHS mice. Notably, the protective effects of G1 were diminished by the GPER blocker G15. GPER may represent a potential therapeutic target for brain injury associated with EHS.

Keywords: neuroprotection; brain injury associated with exertional heat stroke; G protein-coupled estrogen receptor; G1; endoplasmic reticulum stress; neuronal apoptosis

1. Introduction

Exertional heat stroke (EHS) is a condition characterized by a rapid increase in the body's core temperature during intense physical activity in a hot environment, leading to organ damage. Initial symptoms include central nervous system issues such as delirium, epilepsy, and coma, along with severe hyperthermia (core temperature exceeding 40℃) [1, 2]. This can quickly progress to renal failure [3], disseminated intravascular coagulation [4], cardiac failure [5], and multiple organ failure [6], with mortality rates reaching 27% [7]. Despite advancements in EHS treatment over recent decades, clinical outcomes remain suboptimal. The brain is particularly vulnerable to EHS, with brain injury being a major contributor to the high mortality and disability rates associated with this condition [8]. Therefore, research on the mechanisms of central nervous system injury in EHS and on strategies for its prevention and treatment has garnered significant attention.

Significant sex differences in EHS have been reported [9]. Giersch et al. discovered that, within the same military operation, female soldiers had a 48.2% lower probability of EHS than their male counterparts [10]. Garcia et al. identified that sex disparities in EHS are influenced by estrogen [11]. Earlier studies have associated the protective benefits of estrogen with the activation of the nuclear estrogen receptors ERα and ERβ. However, due to the specificity of estrogen as a sex hormone, it cannot be used clinically in men, and it increases the risk of cervical and endometrial cancer in women [12, 13]. Therefore, its clinical use is severely limited. Subsequent studies unveiled a novel estrogen receptor, G protein-coupled estrogen receptor (GPER), which facilitates the rapid non-genomic effects of estrogen through its specific agonist G1 [14, 15]. GPER plays a protective role in various diseases by regulating cell proliferation, apoptosis, and the inflammatory response to hinder tumor progression, suggesting the potential to replace estrogen in the future [16]. Studies have reported that the GPER agonist G1 has neuroprotective effects [17]. However, to our knowledge, whether the GPER agonist G1 can improve EHS-related brain injury has not been reported.

Endoplasmic reticulum stress (ERS) is a critical factor in apoptosis, where disruptions in cellular homeostasis (infection, hypoxia, or high temperature) can lead to an increase in misfolded proteins. In response, the endoplasmic reticulum activates a stress-response mechanism to correct these misfolded proteins, mitigating the effects of external stressors [18]. This helps maintain the endoplasmic reticulum's internal balance, ensuring the smooth functioning of various physiological processes in the body. However, if the stress is too severe or prolonged, the endoplasmic reticulum's regulation of calcium ions may become disrupted, triggering the apoptosis pathway and ultimately cell death [19]. Research indicates that ERS is implicated in the onset and progression of myocardial injury associated with EHS [20].

Because of the brain-protective effect of GPER and the role of ERS in the regulation of EHS, we hypothesized that activating GPER with G1 could potentially suppress ERS, leading to reduction in apoptosis and ultimately mitigating EHS-induced brain injury. Our study aimed to investigate whether the GPER agonist G1 could alleviate EHS-related brain injury by modulating ERS, specifically focusing on its impact on neuronal apoptosis in the hippocampus of EHS mice. Transcriptome gene sequencing was utilized to compare differential gene expression between the hippocampi of healthy mice and those of mice with EHS-induced brain injury. The alterations in these differential genes were subsequently examined at the pathological and protein levels through the utilization of immunofluorescence and Western blot techniques. This study provides new insights into treatment strategies for EHS-related neurodegenerative diseases.

2. Methods

2.1 Animals

Wild-type male C57BL/6J mice, weighing between 25 g and 30 g and aged 10 weeks, were sourced from the Beijing SPF Animal Technology Company (Beijing, China; Permit number SCXK[Jing] 2019-0010). Male mice were selected for this initial mechanistic study because epidemiological and clinical data indicate a markedly higher incidence of exertional heat stroke in males, particularly in military and athletic populations, and because the GPER agonist G1 is of interest as a potential non-feminizing therapeutic agent for male patients. We acknowledge that this choice limits the direct applicability of our findings to females and that future studies should include both sexes to evaluate potential sex-dependent responses. These mice were kept in a regulated setting featuring a 12-h light and 12-h dark cycle, with temperatures maintained at 22–25°C and relative humidity between 40 and 55%. The mice had unrestricted access to food and water. Following a week of acclimatization, 235 mice were randomly divided into five groups: Control (n = 47), EHS (n = 47), EHS + DMSO (n = 47), EHS + G1 (n = 47), and EHS +

G1 + G15 (n = 47).

Anesthesia and Euthanasia: For all surgical procedures and tissue collection, anesthesia was induced by intraperitoneal injection of sodium pentobarbital at a dose of 50 mg/kg. The depth of anesthesia was confirmed by the absence of pedal withdrawal reflex prior to any intervention. All efforts were made to minimize animal suffering. At the end of the experiments, euthanasia was performed by cervical dislocation under deep sodium pentobarbital anesthesia to ensure a painless death. This method is consistent with the American Veterinary Medical Association (AVMA) Guidelines for the Euthanasia of Animals and was approved by our institutional ethics committee.

Ethical Statement: All animal experiments were conducted in strict accordance with the recommendations in the Guide for the Care and Use of Laboratory Animals of the National Institutes of Health. The protocol was reviewed and approved by the Animal Welfare Ethics Committee of the Chinese PLA General Hospital (Approval Number: 2023-X19-15). This study is reported in accordance with the ARRIVE guidelines.

2.2 EHS mouse model

Prior to initiating the preparation model, all mice across each group were acclimated to the artificial climate chamber (Model LTH-575N-01 Shanghai Longyue), a small animal running stage (Model ZS-PT-III Beijing Zhongshi), and a rectal thermonuclear probe (BW-TH1101, Billion, Shanghai, China). Adaptive training was conducted at Tenv 27 ± 0.5℃/RH 55 ± 5%. Mice were placed on a running stage for 2 h daily, maintaining a speed of 10 m/s over a duration of 2 weeks, followed by a 2-day rest period before the start of the experiment. To induce EHS, the chamber was set to high temperature and humidity (39.5℃, 65% RH). The mice were positioned on the treadmill set to a speed of 10 m/s, initiating the forced running protocol. Their behavior was monitored while rectal temperature was recorded every 10 min. A thermometric probe (BW-TH1101, Billion, Shanghai, China) was inserted 2 cm into the rectum of the mice to measure core body temperature (Tc). The model was successfully established when the Tc of the mice reached 42.7°C and loss of consciousness occurred (defined as inability to keep up with the treadmill speed for three consecutive attempts and no response to continuous electrical stimulation for 0.5mA, 2 s, applied to the tail) [20]. All procedures were conducted under strict monitoring and were approved by our institutional animal ethics committee [2023-X19-15]. All follow-up experiments were conducted 24 h after EHS. [21]. The average time for the mice to reach the EHS endpoint (core temperature ≥42.7°C with loss of consciousness) was 95 ± 8 minutes. The acute mortality rate during the EHS induction phase (prior to the 24-hour observation point) was approximately 30%.

2.3 Experimental groups

A total of 235 mice were randomly divided into five distinct groups, with each group consisting of 47 mice. All drugs were administered intraperitoneally immediately after the induction of EHS. The dosing regimen was single administration for all treatments (the initial sample size and the final analysis sample size are presented in Supplementary Material 2 attached). The composition of the groups was: (1) Control group; (2) EHS group, the model group of EHS; (3) EHS + DMSO group, the vehicle group receiving intraperitoneal injection of DMSO (the vehicle consisted of physiological saline with 1% DMSO (v/v). The single injection dose is 0.2 ml, Thermo Fisher Scientific); (4) EHS + G1 group, the cohort consisting of EHS mice was administered an intraperitoneal injection of the GPER-specific agonist G1 (200 µg of G1 was dissolved in physiological saline (0.9% sodium chloride solution) containing 1% DMSO (by volume ratio). Adjust the volume to 200 µL. Final concentration: 1 mg/mL. The single injection dose is 0.2 ml, Sigma-Aldrich) [22]. Additionally, there was a fifth group, labeled as EHS + G1 + G15, which involved EHS mice receiving both the GPER agonist G1 (200 µg of G1 was dissolved in physiological saline (0.9% sodium chloride solution) containing 1% DMSO (by volume ratio). Adjust the volume to 200 µL. Final concentration: 1 mg/mL. The single injection dose is 0.2 ml, Sigma-Aldrich) and the GPER-specific inhibitor G15 (200 µg of G15 was dissolved in physiological saline (0.9% sodium chloride solution) containing 1% DMSO (by volume ratio). Adjust the volume to 200 µL. Final concentration: 1 mg/mL. The single injection dose is 0.2 ml, Sigma-Aldrich) through an intraperitoneal injection.

2.4 Transcriptome sequencing

At the point of sacrifice, hippocampal tissues were swiftly excised and rapidly frozen in liquid nitrogen. RNA extraction was conducted from the hippocampal tissue sections of both the control and EHS groups to facilitate differential expression analysis (Shenzhen, Huada Genome). Gene expression levels were determined utilizing RSEM (v1.3.1), and heatmaps illustrating gene expression variations across samples were created with pheatmap (v1.0.8). In essence, differential expression analysis was conducted using

DESeq2 (v1.4.5), DEGseq42, or PoissonDis with Q-value thresholds of ≤ 0.05 or FDR thresholds of ≤ 0.001. To detect phenotypic changes, enrichment analyses of annotated differentially expressed genes were executed with Phyper, utilizing hypergeometric testing through Gene Ontology (http://www.geneontology.org/) and the Kyoto Encyclopedia of Genes and Genomes (KEGG; https://www.kegg.jp/). The significance levels for terms and pathways were adjusted with the Q-value and a strict threshold (Q-value ≤ 0.05).

2.5 Modified neurological severity score (mNSS)

The modified Neurological Severity Score (mNSS) was used as previously described [23]. The score (0–18) assesses motor function (0–6), sensory response (0–2), beam balance (0–6), and reflexes (0–4). A higher score indicates more severe neurological impairment. All assessments were performed by two investigators blinded to group allocation. The 24-hour time point was selected for subsequent experiments because it represented the peak of neurological deficit in our model (Fig. 1a), consistent with the acute phase of EHS-induced injury reported in prior studies [21].

2.6 Morris water maze (MWM) test

MWM assessments were conducted to evaluate spatial memory and learning capabilities. The maze featured a circular apparatus with a radius of 60 cm and a height of 50 cm, segmented into four sections. An escape platform, measuring 4.5 cm in radius, was submerged 2 cm below the surface at the center of one section. The temperature of the water was kept at 22°C and was colored with titanium dioxide for the mice. The container provided visual cues and was situated in a dimly lit, soundproof room. Directional navigation tests were conducted over 5 consecutive days, with mice released from various starting positions into the water to locate the hidden platform.

Daily, the experiment was conducted four times at 30-min intervals. A computer-controlled video tracking system was utilized to record the duration taken to reach the platform and the swimming trajectory (maximum time allowed: 90 s). Mice were given a direct 15-s window to reach the platform. The escape latency was measured as the duration from the starting point to the platform. On the sixth day, the platform was taken away, and the mice were placed at the end opposite the platform, permitting them to navigate through the maze for 90 s.

2.7 Brain water content

From each group, six mice were chosen at random 24 h post-EHS injury. These mice were anesthetized deeply before being sacrificed, allowing their brains to be weighed right away to establish the wet weight. Following this, the samples were dried at a temperature of 120°C for 24 h and reweighed to ascertain the dry weight. The brain water content (%) was determined using the formula [(wet weight − dry weight)/wet weight] × 100%.

2.8 TUNEL staining

An in-situ cell death assay kit (Roche Molecular Biochemicals) was employed for TUNEL analysis in brain tissue collected 24 h after EHS, adhering to the manufacturer's guidelines. Brain sections were stained and examined with a confocal microscope

(Olympus), and digital images were taken. The TUNEL-positive cells located in the CA1 region (50 µm × 50 µm) of three slides (n = 6) were manually counted for each group. The counting of cells was performed in a blinded fashion using a 20× objective lens.

2.9 Nissl staining

Twenty-four hours post-EHS, sections from the hippocampal region were first handled with 0.01 M phosphate-buffered saline (PBS) before being immersed sequentially in dimethylbenzene I, II, and III at concentrations of 90%, 80%, and 70% for a duration of 5 min each. Following this, the sections were incubated in 5 g of Nissl solution at 37°C for 20 min. After the incubation period, the sections were washed with distilled water and subsequently treated with 95% alcohol for the purpose of color separation. Upon microscopic examination, distinct Nissl bodies were observed. Lastly, the sections were dehydrated using anhydrous alcohol, cleared with xylene, and mounted in neutral balata.

2.10 Immunofluorescence

The hippocampal region's paraffin sections were subjected to immunofluorescence analysis 24 h after exposure to EHS. Dewaxing of the sections was performed using xylene and alcohol, followed by an 8-min treatment with citrate repair solution. Afterward, the sections were rinsed with PBS and incubated in a 1% solution of bovine serum albumin. They were then treated overnight at 4°C with rabbit polyclonal antibodies against caspase-12, GRP78, and CHOP (dilution of 1:500; Abcam, Cambridge, UK) in PBS (dilution of 1:125). Following another wash with PBS, the sections received a 1-h treatment at 37°C with FITC-conjugated anti-rabbit secondary antibody (1:100; Santa Cruz Biotechnology, Dallas, TX, USA). After rinsing with PBS again, the sections were restained with 4′,6-diamidino-2-phenylindole (Sigma-Aldrich) and examined under a confocal laser-scanning microscope (Zeiss, Oberkochen, Germany) for the immunofluorescence staining of caspase-12, CHOP, and GRP78. The average optical densities were calculated using ImageJ (Media Cybernetics, Rockville, MD, USA) by analyzing five high-magnification visual fields per sample, and the fluorescence intensities across groups were statistically assessed.

2.11 Western blotting

Twenty-four hours after exposure to EHS, four mice from each experimental group were euthanized for the purpose of conducting a Western blot assay. The homogenates obtained from the hippocampal region were incubated for 30 min at 4°C and subsequently subjected to centrifugation at 10,450 × g for 15 min to isolate hippocampal proteins. The concentration of proteins in the supernatant was quantified using a protein assay kit. Following this, the proteins were transferred onto a polyvinylidene fluoride membrane (EMD Millipore, Billerica, MA, USA) after they were separated by Tris-glycine denaturing gradient gel electrophoresis. The membrane underwent a blocking step for 1 h at 37°C in Tris-buffered saline with Tween (pH 8.0, 10 mM Tris-HCl, 150 mM NaCl, and 0.2% Tween 20), and then incubated overnight at 4°C with the following antibodies: rabbit monoclonal anti-GRP78 (1:500; Abcam), mouse monoclonal anti-CHOP (1:500; Abcam), and rabbit polyclonal anti-caspase-12 (1:1000; Abcam). The blot was washed with Tris-buffered saline containing Tween and then exposed to a horseradish peroxidase-conjugated secondary antibody (anti-rabbit or anti-mouse; 1:20,000; Santa Cruz Biotechnology) for 2 h at room temperature. Detection of staining was performed using enhanced chemiluminescence (GE Healthcare, Chicago, IL, USA), and the target protein bands were identified through an enhanced chemiluminescence kit paired with X-ray film. Grayscale values of the bands were quantified and normalized relative to the corresponding β-actin levels from the same sample.

2.12 Statistical analysis

Data analysis and blinded observation were conducted using GraphPad Prism (version 8.0, San Diego, CA, USA). Results are presented as mean ± standard error of the mean. To assess differences between the five experimental groups, a two-way analysis of variance followed by Tukey's post-hoc test was employed. A P-value of less than 0.05 was deemed statistically significant.

3. Results

3.1 EHS induces brain injury

The mNSS was utilized to monitor neurobehavioral alterations in mice at 6 h, 12 h, 24 h, 48 h, and 72 h following EHS. The higher the score, the more severe the injury. A significantly higher score was observed at 24 h after EHS ($p < 0.05$; Fig. 1a).

We focused on 24 h after EHS as the study time point based on the degree of nerve injury in mice. The selection of the 24-hour time point was primarily based on our longitudinal mNSS data (Fig. 1a), which indicated that the most severe neurological deficits occurred at 24 hours post-EHS. Similarly, transcriptome sequencing of mouse hippocampal tissues was performed 24 h after EHS to identify genes and pathways contributing to EHS pathology. Transcriptome sequencing revealed that *GPER* is a potentially important gene in the occurrence and development of EHS-related brain injury (Fig. 1b).

KEGG pathway enrichment analysis was performed using RNA sequencing data to investigate potential cell death patterns in hippocampal tissue cells after EHS-induced brain injury. The results showed that the ERS pathway, as one of the pathways affecting cell death, may play an important role in brain injury after EHS. Beyond the ERS pathway, KEGG enrichment analysis of differentially expressed genes also highlighted significant alterations in pathways related to IL-17 signaling pathway, FoxO signaling pathway, P53 signaling pathway, and apoptosis, consistent with the multifaceted cellular stress response induced by EHS (Fig. 1c).

3.2 G1 relieves EHS-induced brain injury in mice

Compared with the control group, there was a notable rise in the mNSS observed in the EHS group ($p < 0.05$; Fig. 2a). Nevertheless, no significant difference in mNSS was found between the EHS + DMSO and EHS groups. When contrasted with the EHS group, the mNSS showed a significant decrease in the EHS + G1 group ($p < 0.05$; Fig. 2a). In juxtaposition to the EHS + G1 group, the mNSS experienced a significant increase in the EHS + G1 + G15 group ($p < 0.05$; Fig. 2a). About 24 h following EHS, a significant increase in brain water content was recorded in both the EHS and EHS + DMSO groups when compared with the control group ($p < 0.05$; Fig. 2b). Additionally, the brain water content was significantly lower in the EHS + G1 group compared with the EHS group ($p < 0.05$; Fig. 2b). However, there was no significant difference in brain water content between the EHS and EHS + DMSO groups ($p < 0.05$; Fig. 2b). Finally, the brain water content significantly rose in the EHS + G1 + G15 group when compared with the EHS + G1 group ($p < 0.05$; Fig. 2b).

3.3 G1 relieves EHS-induced cognitive dysfunction in mice

The Morris Water Maze (MWM) test was employed to assess the impact of brain injury induced by EHS in mice. In the spatial acquisition training phase of the MWM, the mice's capability to find the hidden platform improved with ongoing training sessions. The comparisons of latency between the groups for each day did not show significant differences ($p = 0.24$; Fig. 3a). Both the probe test and working memory assessment were conducted 24 h post-EHS. During the probe test, the variations in swimming speed and distance among the five groups were not statistically significant, suggesting that any performance discrepancies were not a result of spontaneous activity or motor capabilities ($p > 0.05$; Fig. 3b). The time taken to reach the platform was considerably longer for the EHS group compared with the control group, whereas it was significantly reduced for the EHS + G1 group when juxtaposed with the EHS group. Specifically, the latency to locate the platform was significantly greater in the EHS group than in the control group ($p < 0.001$; Fig. 3c) and notably less in the EHS + G1 group compared with the EHS group ($p < 0.05$; Fig. 3d). This implies that mice subjected to EHS took more time to identify the hidden platform, indicating a compromised ability to utilize reference cues during memory training after the model was developed, an impairment that G1 was effective in alleviating. Moreover, the proportion of swimming distance in the target quadrant ($p < 0.05$; Fig. 3e) and the frequency of crossings at the platform location ($p < 0.05$; Fig. 3f) were diminished in the EHS group relative to the control group, indicating that EHS adversely affected the memory capability of the mice. Additionally, compared with the EHS group, the aforementioned metrics showed improvement in the EHS + G1 group, with all significant differences noted aside from the percentage of swimming distance in the target quadrant ($p < 0.05$; Fig. 3g). In the working memory evaluation, the outcomes on the first and second days were notably similar. The time taken to reach the platform site was notably extended for the EHS group compared with the control group, while it was reduced in the EHS + G1 group relative to the EHS group. The working memory assessment indicated the mice's short-term learning and memory capabilities, implying that G1 has the potential to enhance brain damage caused by EHS. Additionally, this protective benefit provided by G1 could be inhibited by the GPER-specific inhibitor G15.

3.4 G1 alleviates EHS-induced neuronal damage in the hippocampus

Nissl staining (Fig. 4a) illustrated neuronal in the hippocampus. The groups receiving EHS and EHS + G1 showed a notable decrease in the count of Nissl bodies in comparison to the control group ($p < 0.05$; Fig. 4c), whereas the EHS + G1 group showed an increase in Nissl bodies compared with the EHS and EHS + DMSO groups ($p < 0.05$; Fig. 4c). This protective effect was receptor-dependent, as co-administration of the GPER receptor antagonist G15 significantly attenuated the neuroprotective effects of G1 ($p < 0.05$; Fig. 4c). A non-significant difference was observed between the EHS group and the EHS + DMSO group ($p > 0.05$; Fig. 4c). TUNEL staining (Fig. 4b) illustrated neuronal death in the hippocampus. Compared with those in the control group, significantly more TUNEL-positive cells were observed in the EHS and EHS + DMSO groups ($p < 0.0001$; Fig. 4d). However, the number of TUNEL-positive cells was significantly lower in the EHS + G1 group than in the EHS and EHS + DMSO groups ($p < 0.0001$; Fig. 4d). A non-significant difference was observed between the EHS group and the EHS + PBS group ($p > 0.05$; Fig. 4d). G15 appeared to counteract the neuroprotective effects of G1. TUNEL staining showed that the apoptotic cell count in the EHS + G1 + G15 was similar to that in the EHS ($p = 0.64$) but higher than that in the EHS + G1 ($p < 0.001$; Fig. 4d).

3.5 G1 inhibits ERS, thereby reducing neuronal apoptosis

We examined the apoptotic protein caspase-3 in the hippocampus and key proteins in ERS, such as caspase-12, CHOP, and GRP78. This brain region is primarily affected by apoptosis following an injury.

Immunofluorescence analysis indicated a notable rise in caspase-3 levels within the EHS group (Fig. 5a). When comparing the groups, the quantity of activated apoptotic cells was significantly elevated in both the EHS and EHS + DMSO groups relative to the control group. However, there was no significant difference in the number of activated apoptotic cells between the EHS and EHS + DMSO groups. In contrast, the activation of apoptosis was markedly diminished in the EHS + G1 group compared to the EHS and EHS + DMSO groups ($p < 0.001$; Fig. 5b). Co-treatment with G15 negated this effect, leading to significantly elevated caspase-3 levels compared to those achieved with G1 alone ($p < 0.05$; Fig. 5b). Additionally, enzyme-linked immunosorbent assay alongside Western blotting (WB) confirmed a significant increase in levels of caspase-12, CHOP, and GRP78 ($p < 0.001$; Fig. 5c) in the hippocampal region of the EHS and EHS + DMSO groups when contrasted with the Control group. Treatment with G1 significantly reduced the levels of caspase-12 ($p < 0.05$; Fig. 5c), CHOP ($p < 0.05$; Fig. 5c), GRP78 ($p < 0.05$; Fig. 5c), and caspase-3 ($p < 0.05$; Fig. 4c) in the EHS + G1 group. Notably, G15 returned the apoptosis levels to those comparable to baseline EHS (caspase-12: $p = 0.08$; CHOP: $p = 0.10$; GRP78: $p = 0.1$; caspase-3: $p = 0.07$). No significant differences were found in the levels of caspase-12, CHOP, GRP78, or caspase-3 among the EHS, EHS + DMSO, and EHS + G1 + G15 groups.

4. Discussion

Brain injury is a common complication of EHS, which may lead to brain death and nerve damage, such as decreased learning and memory abilities [24]. However, the mechanism through which EHS induces brain injury remains unclear. Through animal experiments in this study, we established that EHS can lead to brain injury, peaking at 24 h post-EHS. KEGG enrichment analysis of altered genes confirmed that GPER- and ERS-mediated apoptosis play key roles in EHS-related brain injury.

Based on the results of transcriptome sequencing and prior research, we hypothesized that the GPER-specific agonist G1 could potentially mitigate brain function impairments induced by EHS by inhibiting ERS-mediated apoptosis in the hippocampus of EHS mice. Consequently, G1 was administered immediately following EHS, with dosage selection primarily informed by existing studies on G1 in various animal models. Furthermore, considering that G1 is a biologically active compound capable of crossing the blood-brain barrier through multiple mechanisms [25,26], we selected intraperitoneal injection as the method of administration. Ultimately, this study demonstrated that G1 can alleviate brain impairments in EHS mice and reduce ERS-mediated apoptosis.

Exposure to environmental heat can lead to cognitive deficits [27]. MWM tests assess learning and memory in rodents and show that environmental heat exposure causes brain deficits. Here, MWM tests indicated a decline in cognitive abilities, particularly at 24 h, emphasizing the immediate impact of EHS-induced brain injury and the need for early intervention.

Previous studies have confirmed the diverse biological functions of G1, including anti-apoptotic, tumor-suppressing, and anti-inflammatory properties, as well as its role in ameliorating organ damage from various diseases. Researchers have increasingly recognized the significance of G1 in neuroprotection against neurodegenerative diseases and brain injuries [28–30]. However, the role and mechanisms of G1 in EHS-induced brain dysfunction are understudied. This study showed the effectiveness of G1 in alleviating EHS-induced brain impairments and explored its specific mechanisms.

We investigated the neuroprotective and anti-apoptotic effects resulting from the activation of GPER in an animal model of EHS-related brain injury. Our findings indicated that GPER activation led to reduction in neuronal apoptosis and enhancement in neurological performance. Furthermore, we observed a significant decrease in apoptosis, as evidenced by lower expression levels of ERS-related proteins, including GRP78, CHOP, and caspase-12, as well as the apoptosis-related protein caspase-3 in the EHS+G1 group 24 h post-EHS. The activation of GPER inhibited apoptosis via the suppression of the ERS-mediated apoptotic pathway. The measurement of brain water content is a direct indicator of cerebral edema [31], a critical pathological feature of severe brain injury that contributes to increased intracranial pressure and secondary neuronal damage [32]. The significant increase in brain water content was observed 24 hours after EHS. The reduction in edema by G1 treatment suggests that GPER activation may help stabilize vascular integrity or mitigate the inflammatory cascade driving fluid extravasation, contributing to its overall neuroprotective effect. Conversely, the protective effect of GPER on EHS was negated by the application of the GPER inhibitor G15. We acknowledge that a detailed time-course analysis of ERS activation (e.g., p-PERK, sXBP1) and apoptosis across earlier and later time points is necessary to fully define the therapeutic window and temporal dynamics of G1 action. This constitutes an important direction for our future work.

G1 and G15 serve as selective inhibitors and agonists of GPER, respectively. Their identification has enabled functional investigations of GPER in various animal tissues and cells [33]. G1 has advanced to Phase 1 clinical trials aimed at treating cancer [34]. Numerous studies have indicated the protective functions of GPER in conditions like cerebral ischemia-reperfusion injury and renal ischemia-reperfusion injury [35, 36]. Furthermore, GPER plays a role in hindering breast cancer progression via the JNK/c-

Jun/p53/Noxa signaling pathway [37]. Observations of GPER’s neuroprotective capabilities have been made in vitro in contexts such as ischemic stroke, experimental stroke, glioma, and neuroblastoma cells [38, 39]. This study's findings revealed that administering the GPER agonist G1 led to considerable improvements in neurobehavioral functions and a decrease in brain water content in EHS mice. Other researchers have also indicated that G1 can enhance the permeability of the blood-brain barrier following global cerebral ischemia in mice and decrease neuronal apoptosis in EHS mice [40]. These results imply that the activation of GPER may be a promising avenue for treating neurodegenerative disorders and injuries to the central nervous system. Consequently, this investigation focused on the protective effects resulting from GPER activation against EHS injury and examined the underlying mechanisms driving these neuroprotective effects. Since GPER was identified in the brain, some researchers have proposed that it functions as a typical estrogen receptor, providing neuroprotection, particularly in cases of ischemia-reperfusion injury. The GPER agonist utilized in this study (G1) does not engage with traditional nuclear receptors. As a result, it could be applicable for male patients as it avoids the negative effects linked to hormone replacement therapy [41]. Furthermore, the results from Nissl staining revealed clear pyramidal neurons in the hippocampus along with cytoplasmic staining following G1 treatment. Our results strongly suggest that treatment with G1 can mitigate neurological deficits. The therapy specifically reduced damage in the EHS + G1 group. Nevertheless, these beneficial effects were negated by the inclusion of the GPER antagonist G15, thereby substantiating the significant role of GPER in mediating estrogen receptor activities.

Although our research has determined that G1 may be a new drug for improving brain injury caused by EHS, some limitations deserve careful explanation and further study. First, although we demonstrated that G1 alleviates neuronal apoptosis in the hippocampus by inhibiting ERS, the exact molecular mechanism linking G1 activation to ERS remains unresolved. Second, this study evaluated relevant indicators only at 24 h after EHS, which was the final time point for observing brain injury. The chronological sequence of EHS occurrence and the neuroprotective effect of G1 remains unclear. Furthermore, it is currently unclear whether other forms of cell death, such as inflammatory neutrophil death and pyro ptosis, can lead to EHS-related brain injury. The interaction with G1 awaits further study. Third, the experiment included only animal models, and the lack of human hippocampal verification limited the generalizability of the results. Future research on brain samples from patients with heatstroke or human neuron models will enhance clinical relevance. Fourth, this study was conducted exclusively in male mice. While this aligns with the higher reported incidence of EHS in males and focuses on a potential therapeutic pathway for male patients, it precludes any understanding of sex-specific responses. The protective effects of GPER activation and its interaction with ERS may differ in females due to varying basal estrogen levels and receptor expression. Future studies must include female animals to determine whether G1-mediated neuroprotection is sex-dependent. Fifth, the experimental design did not include control groups receiving G1 or G1+G15 without EHS. The inclusion of such groups would have formally ruled out any confounding effects of the compounds themselves on our measured outcomes. Future dose-response and safety studies should incorporate these controls. Sixth, the experimental design did not include a sham surgery group. If such a control group were included, it would formally eliminate any possible interference effects of the sham surgery on our measurement results. In future research, we will incorporate this in our study. Furthermore, the study design, which utilized separate cohorts for behavioral and molecular analyses, did not permit correlation analysis at the individual animal level between the extent of apoptosis reduction and the degree of cognitive improvement. Future studies employing within-subject longitudinal designs could more robustly establish this direct relationship.

5. Conclusion

Our results illustrate a causal chain in which EHS-induced ERS leads to neuronal apoptosis. G1 interrupts this cascade by inhibiting ERS, thereby protecting neuronal integrity in a GPER-dependent manner. These insights suggest that G1, or GPER-targeting strategies, could represent a promising therapeutic direction for mitigating EHS-related brain damage and highlight the potential relevance of this pathway in other central nervous system diseases involving ERS. However, to establish direct mechanistic causality, future studies should further explore the following strategies: using genetic knockdown or knockout approaches to clarify the necessity of GPER in the observed neuroprotection; delving into upstream ERS signaling pathways (such as PERK, IRE1α, and ATF6) to elucidate the specific mechanisms by which GPER activation regulates ERS; systematically conducting time-course and dose-response studies to define the temporal window and concentration-dependent effects of G1; and incorporating female animal models to comprehensively assess sex-dependent differences. Such work will help strengthen the mechanistic link between GPER activation and ERS inhibition in EHS-induced brain injury at the molecular and pathway levels. This study provides a preliminary foundation for further exploration of the mechanisms through which GPER modulation alleviates central nervous system injury after EHS and supports the need for subsequent preclinical and translational studies.

References

[1] Bouchama, A. et al. Classic and exertional heatstroke. *Nat. Rev. Dis. Primers* **8**, 8 (2022).

[2] Bouchama, A. & Knochel, J. P. Heat stroke. *N. Engl. J. Med.* **346**, 1978–1988 (2002).

[3] Wang, C. et al. Association of D-dimer and acute kidney injury associated with rhabdomyolysis in patients with exertional heatstroke: an over 10-year intensive care survey. *Ren. Fail.* **43**, 1561–1568 (2021).

[4] DeGroot, D. W., Litchfield, A. C., Blodgett, C. A., Rhodehouse, B. B. & Hudson, K. P. Chain of survival for a severe exertional heat stroke casualty. *J. Appl. Physiol. (1985)* **138**, 699–705 (2025).

[5] Chao, C. M. et al. Myocardial structure and functional alterations in a preclinical model of exertional heat stroke. *Life Sci.* **323**, 121640 (2023).

[6] Lorenz, E., Herold, J., Lodes, U. & Meyer, F. Fatal heat stroke based on foudroyant irreversible multiple organ dysfunction in German summer. *Innov. Surg. Sci.* **8**, 129–134 (2023).

[7] Garcia, C. K., Renteria, L. I., Leite-Santos, G., Leon, L. R. & Laitano, O. Exertional

heat stroke: pathophysiology and risk factors. *BMJ Med.* **1**, e000239 (2022).

[8] Xie, J. et al. Exertional heat stroke-induced changes in gut microbiota cause cognitive impairment in mice. *BMC Microbiol.* **24**, 134 (2024).

[9] Goodwin, K. C., Giersch, G. E. W., Murray, T. A., DeGroot, D. W. & Charkoudian, N. Sex differences in biomarkers of end-organ damage following exertional heat stroke in humans. *J. Appl. Physiol. (1985)* **137**, 1434–1445 (2024).

[10] Giersch, G. E. W., Garcia, C. K., Stachenfeld, N. S. & Charkoudian, N. Are there sex differences in risk for exertional heat stroke? A translational approach. *Exp. Physiol.* **107**, 1136–1143 (2022).

[11] Garcia, C. K. et al. Sex-dependent responses to exertional heat stroke in mice. *J. Appl. Physiol. (1985)* **125**, 841–849 (2018).

[12] Shen, B. et al. Estrogen-induced extracellular calcium influx promotes endometrial cancer progress by regulating lysosomal activity and mitochondrial ROS. *Front. Med. (Lausanne)* **9**, 835700 (2022).

[13] Xi, Y., Zheng, P., Xi, W. & Fu, T. Exploring the impact of estrogenic endocrine disruptors on cervical cancer progression: A transcriptome analysis and prognostic model development. *Ecotoxicol. Environ. Saf.* **285**, 117025 (2024).

[14] Diaz-Zegarra, L. A. et al. Electrophysiological changes induced by G1, the selective agonist of the G-protein coupled estrogen receptor (GPER), in the clip-TAC mice model. A new potential cardioprotective mechanism. *Life Sci.* **379**, 123873 (2025).

[15] Xu, S., Yu, S., Dong, D. & Lee, L. T. O. G protein-coupled estrogen receptor: a potential therapeutic target in cancer. *Front. Endocrinol.* **10**, 725 (2019).

[16] Kutuk, O. & Kaplan, A. Phytoestrogen signal pathways and estrogen signaling in ovarian cancer: a narrative review. *Phytother. Res.* **39**, 3601–3612 (2025).

[17] Kilanowski-Doroh, I. M. et al. Ovariectomy-induced arterial stiffening differs from vascular aging and is reversed by GPER activation. *Hypertension* **81**, e51–e62 (2024).

[18] Karamali, N. et al. Pathophysiology of endoplasmic reticulum stress and the potential role of dexmedetomidine as a modulator. *BioFactors* **51**, e70022 (2025).

[19] Lee, J. et al. Roridin E and satratoxin H, macrocyclic trichothecene mycotoxins, induce endoplasmic reticulum stress-dependent apoptosis through ribosome interaction in B16 mouse melanoma cells. *Bioorg. Chem.* **164**, 108842 (2025).

[20] Zhang, B. Y. et al. L-carnitine ameliorates myocardial injury by alleviating endoplasmic reticulum stress via inhibition of PERK pathway in exertional heatstroke rats. *Heliyon* **10**, e40502 (2024).

[21] Song, R. et al. A mouse model of exertional heatstroke-related acute kidney injury. *Ann. Transl. Med.* **10**, 276 (2022).

[22] Sharma, G. et al. Preclinical efficacy of the GPER-selective agonist G-1 in mouse models of obesity and diabetes. *Sci. Transl. Med.* **12**, eaau5956 (2020).

[23] Qian, Y. et al. SRGN amplifies microglia-mediated neuroinflammation and exacerbates ischemic brain injury. *J Neuroinflammation.* **21**, 35 (2024).

[24] Li, J. et al. Heat acclimation defense against exertional heat stroke by improving the function of preopticTRPV1 neurons. *Theranostics* **15**, 1376–1398 (2025).

[25] Waters, E. M. et al. G-protein-coupled estrogen receptor 1 is anatomically

positioned to modulate synaptic plasticity in the mouse hippocampus. *J Neurosci*. 35, 2384-2397 (2015).

[26] Peng, J., He, J., Hu, X. & Xia, Y. GPR30 alleviated subarachnoid hemorrhage-induced blood-brain barrier dysfunction by activating the PI3K/Akt and Nrf2/HO-1 pathways. *Am J Physiol Cell Physiol.* 327, C65-C73 (2024).

[27] Larson, P. S. et al. Long-term exposure to extreme heat and cold and cognitive decline in older adults: results from the Reasons for Geographic and Racial Differences in Stroke (REGARDS) cohort. *Environ. Res.* **283**, 121984 (2025).

[28] Fu, Z. et al. GPER agonist G-1 activates YAP to induce apoptosis in breast cancer cells. *J. Steroid Biochem. Mol. Biol.* **248**, 106693 (2025).

[29] Mohammad-Sadeghipour, M. et al. G protein-coupled estrogen receptor reduces the breast cancer cell survival by regulating the IRE1α/miR-17-5p/TXNIP pathway. *J. Steroid Biochem. Mol. Biol.* **252**, 106770 (2025).

[30] Wowui, P. I. et al. Estrogen via GPER downregulated HIF-1a and MIF expression, attenuated cardiac arrhythmias, and myocardial inflammation during hypobaric hypoxia. *Mol. Med.* **31**, 107 (2025).

[31] Kozler, P., Marešová, D. & Pokorný, J. Determination of brain water content by dry/wet weight measurement for the detection of experimental brain edema. *Physiol Res.* 71, S277-S283 (2022).

[32] Alsbrook, D. L. et al. Neuroinflammation in Acute Ischemic and Hemorrhagic Stroke. *Curr Neurol Neurosci Rep.*23, 407-431 (2023).

[33] Chou, Y. S. et al. G-protein-coupled estrogen receptor-1 facilitates chondrocyte

proliferation in pubertal epiphyseal growth plate via PTHrP/Ihh regulation. Bone Joint Res. 14, 589–600 (2025).

[34] Langdon, S. P., Herrington, C. S., Hollis, R. L. & Gourley, C. Estrogen signaling and its potential as a target for therapy in ovarian cancer. Cancers 12, 1647 (2020).

[35] Chang, Y. et al. G protein-coupled estrogen receptor activation improves contractile and diastolic functions in rat renal interlobular artery to protect against renal ischemia reperfusion injury. *Biomed. Pharmacother.* **112**, 108666 (2019).

[36] Han, Z. W. et al. GPER agonist G1 suppresses neuronal apoptosis mediated by endoplasmic reticulum stress after cerebral ischemia/reperfusion injury. *Neural Regen. Res.* **14**, 1221–1229 (2019).

[37] Cirillo, F. et al. GPER deletion triggers inhibitory effects in triple negative breast cancer (TNBC) cells through the JNK/c-Jun/p53/Noxa transduction pathway. *Cell Death Discov.* **9**, 353 (2023).

[38] Wang, S. et al. Neuronal GPER participates in genistein-mediated neuroprotection in ischemic stroke by inhibiting NLRP3 inflammasome activation in ovariectomized female mice. *Mol. Neurobiol.* **59**, 5024–5040 (2022).

[39] Yu, Z. et al. Icaritin inhibits neuroinflammation in a rat cerebral ischemia model by regulating microglial polarization through the GPER-ERK-NF-κB signaling pathway. *Mol. Med.* **28**, 142 (2022).

[40] Lu, D. et al. Activation of G protein-coupled estrogen receptor 1 (GPER-1) ameliorates blood-brain barrier permeability after global cerebral ischemia in

ovariectomized rats. *Biochem. Biophys. Res. Commun.* **477**, 209–214 (2016).

[41] Upadhayay, S. et al. Involvement of the G-protein-coupled estrogen receptor-1 (GPER) signaling pathway in neurodegenerative disorders: a review. *Cell. Mol. Neurobiol.* **43**, 1833–1847 (2023).

Acknowledgements: The authors extend their sincere thanks to Zhi Dai, Dongxu Qian, and non-author contributors for their assistance with data collection, technical support, and critical feedback.

Author contributions: Conceptualization: Feihu Zhou Ziwei Han; Data curation: Xiaochen Wang; Formal analysis: Jiansong Guo; Investigation: Chao Liu; Methodology: Jie Hu; Project administration: Zhi Mao; Resources: Feihu Zhou: Supervision: Feihu Zhou; Validation: Yan Shen; Visualization: Baisheng Sun; Writing – original draft: Ziwei Han; Writing – review & editing: Feihu Zhou.

Data Availability: The transcriptome sequencing data generated and analyzed during the current study are available in the National Center for Biotechnology Information (NCBI) under the BioProject number PRJNA1224851. All other data supporting the findings of this study are available from the corresponding author upon reasonable request.

Funding: The authors declare that no funds, grants, or other support were received during the preparation of this manuscript

Competing Interests: The authors declare no competing interests.

Ethics Approval: All animal procedures adhered to the guidelines of the Animal Welfare

Ethics Committee of the Chinese PLA General Hospital (2023-X19-15).

Consent to Participate: Not applicable.

Consent to Publish: Not applicable.

Figure legends

Fig. 1 Effects of EHS-induced brain injury in mice and transcriptome sequencing analysis of hippocampal tissues and potential candidate genes

(a) mNSS behavioral assessment in mice. (b) A clustered heatmap illustrating the average logarithmic values of genes that were differentially expressed in the hippocampal tissue of mice 24 h following EHS. (c) Analyses for pathway enrichment in Kyoto Encyclopedia of Genes and Genomes and Gene Ontology concerning differentially expressed genes in hippocampal tissue of mice. Values are compared to their corresponding control groups. Data are shown as mean ± standard deviation (behavioral mNSS: n = 12; transcriptome sequencing: n = 5). *P < 0.05, vs. Control group; #P < 0.05, vs. EHS (6h) group. EHS refers to exertional heat stroke; mNSS is the modified neurological severity score.

Fig. 2 G1 relieves EHS-induced brain injury in mice

(a) mNSS in the five groups. (b) Brainstem wet-to-weight ratio (degree of brain edema). Data are expressed as mean ± standard deviation (n = 6). *P < 0.05, vs. EHS group; #P < 0.05, vs. EHS + G1 + G15 group; DMSO, dimethyl sulfoxide; EHS, exertional heat stroke; G1, GPER-specific agonist; G15, GPER-specific blocker; mNSS, modified Neurological Severity Score

Fig. 3 G1 relieves EHS-induced cognitive dysfunction in mice

(a) Mouse trajectory representation in the probe test for the five groups. (b) Representative paths to the novel platform during working memory evaluation. (c) Duration needed to reach the platform during the 5 days of practice. (d) Speed of swimming. (e) Proportion of distance covered in the quadrant where the platform was located. (f) Latency to the platform. (g) Number of times the mice crossed the platform location during the probe test. Data are expressed as mean ± standard deviation (n = 12). *$P < 0.05$, vs. EHS group; #$P < 0.05$, vs. EHS + G1 + G15 group; DMSO, dimethyl sulfoxide; EHS, exertional heat stroke; G1, GPER-specific agonist; G15, GPER-specific blocker

Fig. 4 G1 alleviates EHS-induced neuronal damage in the hippocampus

(a) Nissl staining showing neuronal morphological changes (scale bar = 100 µm, top; 50 µm, bottom). (b) TUNEL staining demonstrating cell death in the hippocampus (scale bar = 100 µm, top; 50 µm, bottom). (c) Percentage of Nissl-positive cells. (d) Percentage of TUNEL-positive cells. Data are expressed as mean ± standard deviation (n = 4). *$p < 0.05$ vs. EHS group; #$p < 0.05$, vs. EHS + G1 + G15 group. DMSO, dimethyl sulfoxide; EHS, exertional heat stroke; G1, GPER-specific agonist; G15, GPER-specific blocker

Fig. 5 G1 inhibits endoplasmic reticulum stress-induced apoptosis, thereby preventing EHS-related brain damage

(a) Representative images (scale bar = 50 μm) of caspase-3 in the hippocampal area. (b) The number of caspase-3–positive cells in the hippocampal area (n = 4). (c) Representative Western blot bands of Caspase-3, Caspase-12, GRP78, CHOP, and β-actin from hippocampal lysates. Lanes: Control, EHS, EHS+DMSO, EHS+G1, EHS+G1+G15. (d–g) Optical densities of the protein bands were quantitatively analyzed and normalized to the loading control β-actin (n = 4). EHS, exertional heat stroke. Data are expressed as mean ± standard deviation. *$P < 0.05$, control group vs. EHS group; #$p < 0.05$, EHS group versus EHS + G1 group; DMSO, dimethyl sulfoxide; EHS, exertional heat stroke; G1, GPER-specific agonist; G15, GPER-specific blocker

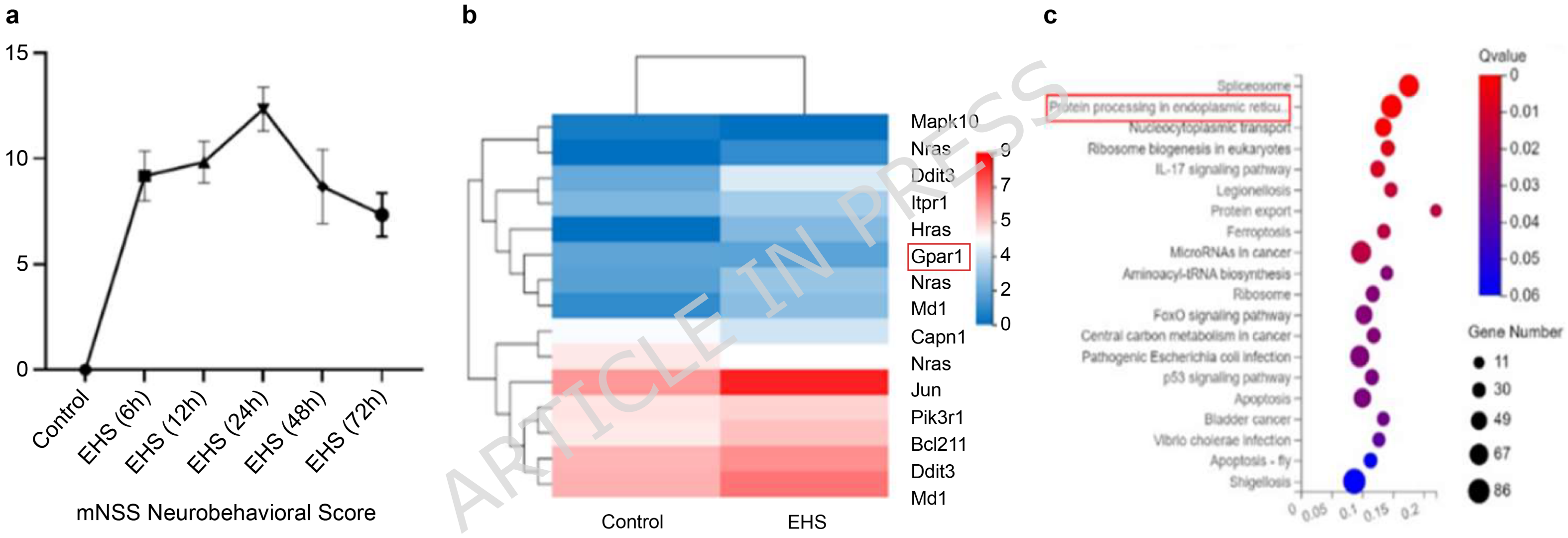
a
15
10
5
0
Control
EHS (6h)
EHS (12h)
EHS (24h)
EHS (48h)
EHS (72h)
mNSS Neurobehavioral Score
b
Mapk10
Nras
Ddit3
Itpr1
Hras
Gpar1
Nras
Md1
Capn1
Nras
Jun
Pik3r1
Bcl211
Ddit3
Md1
9
7
5
4
2
0
Control
EHS
c
Spliceosome
Protein processing in endoplasmic reticu...
Nucleocytoplasmic transport
Ribosome biogenesis in eukaryotes
IL-17 signaling pathway
Legionellosis
Protein export
Ferroptosis
MicroRNAs in cancer
Aminoacyl-tRNA biosynthesis
Ribosome
FoxO signaling pathway
Central carbon metabolism in cancer
Pathogenic Escherichia coli infection
p53 signaling pathway
Apoptosis
Bladder cancer
Vibrio cholerae infection
Apoptosis - fly
Shigellosis
0
0.05
0.1
0.15
0.2
Qvalue
0
0.01
0.02
0.03
0.04
0.05
0.06
Gene Number
11
30
49
67
86

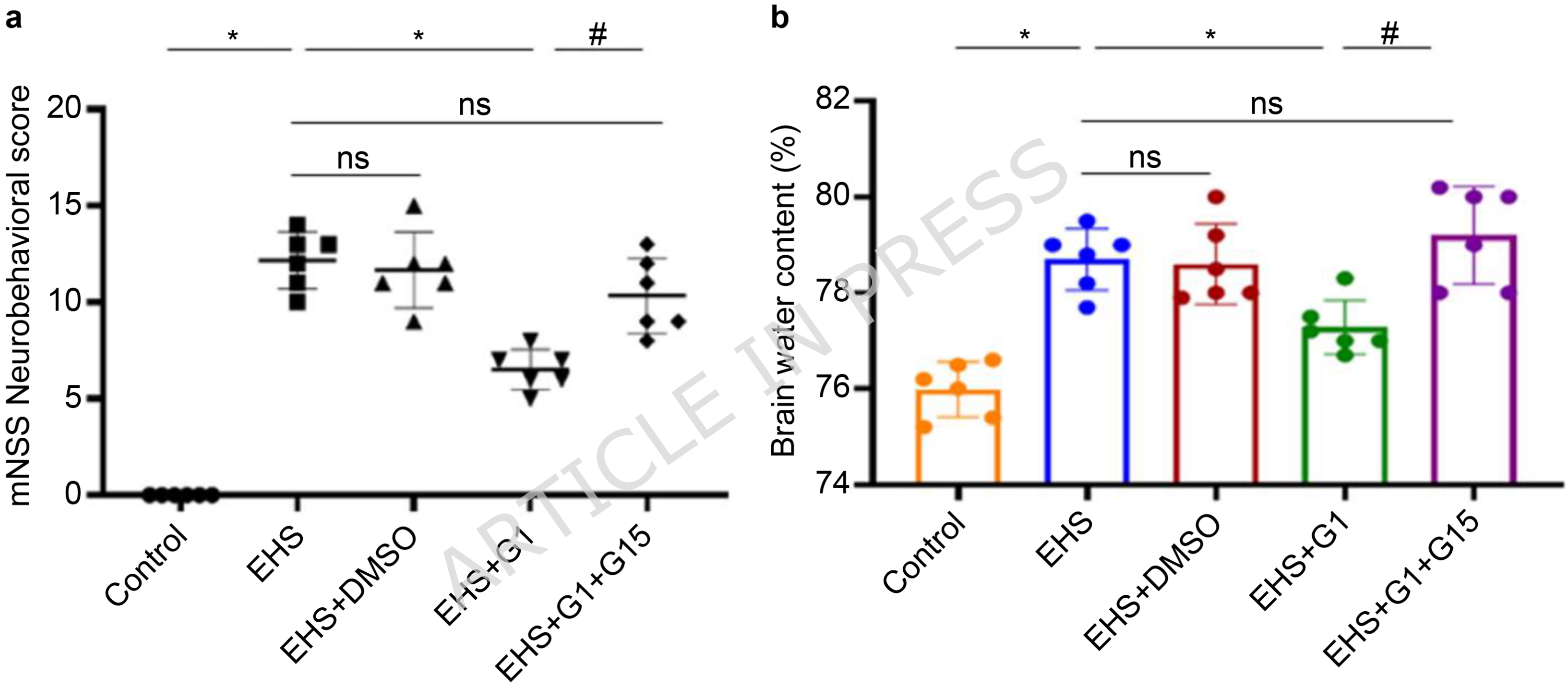
a
*
*
#
ns
ns
mNSS Neurobehavioral score
20
15
10
5
0
Control
EHS
EHS+DMSO
EHS+G1
EHS+G1+G15
b
*
*
#
ns
ns
Brain water content (%)
82
80
78
76
74
Control
EHS
EHS+DMSO
EHS+G1
EHS+G1+G15

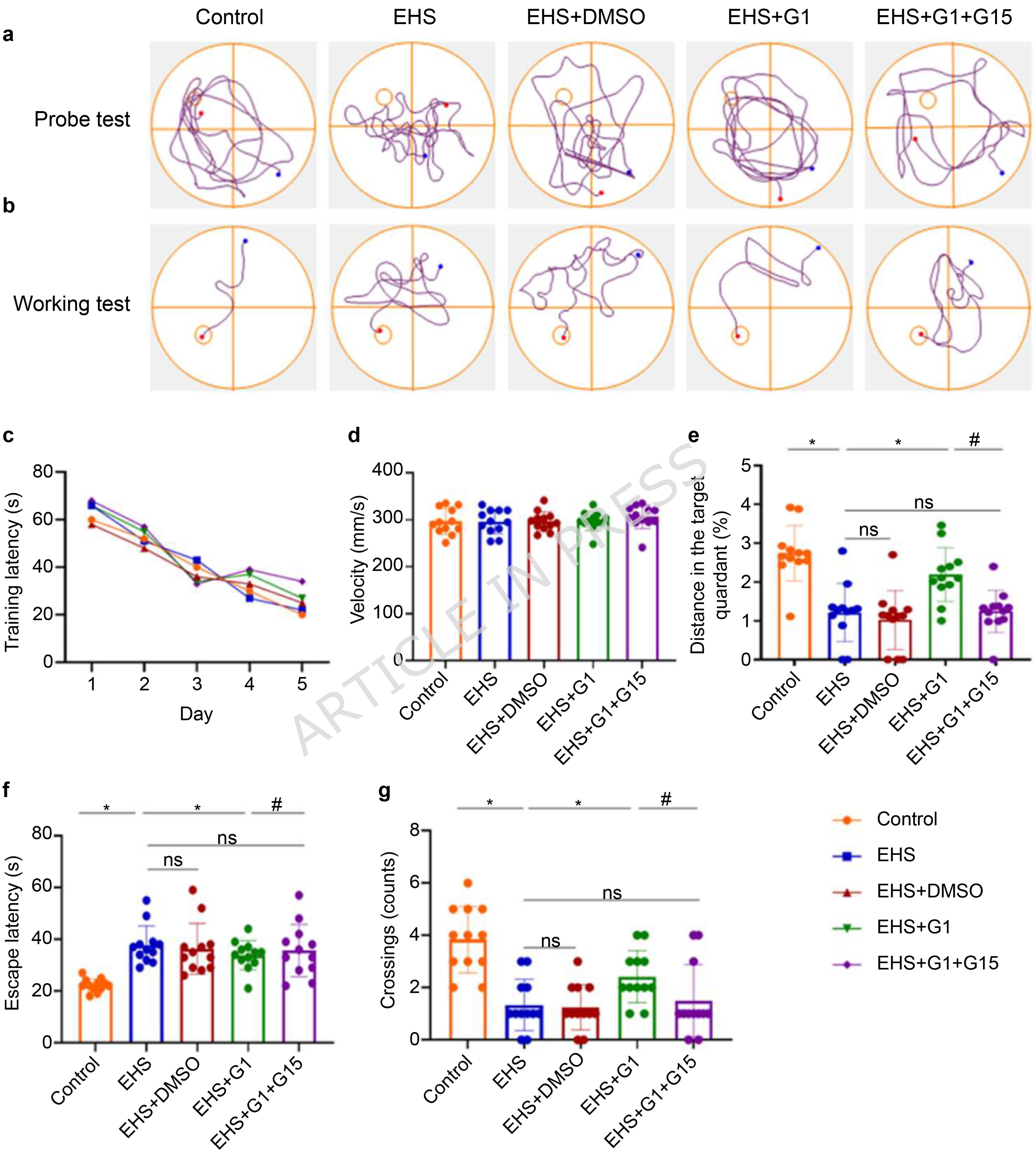
a
b
Control
EHS
EHS+DMSO
EHS+G1
EHS+G1+G15
Probe test
Working test
c
Training latency (s)
0
20
40
60
80
1
2
3
4
5
Day
d
Velocity (mm/s)
0
100
200
300
400
e
Distance in the target quardant (%)
0
1
2
3
4
5
*
*
#
ns
ns
f
Escape latency (s)
0
20
40
60
80
*
*
#
ns
ns
g
Crossings (counts)
0
2
4
6
8
*
*
#
ns
ns
Control
EHS
EHS+DMSO
EHS+G1
EHS+G1+G15

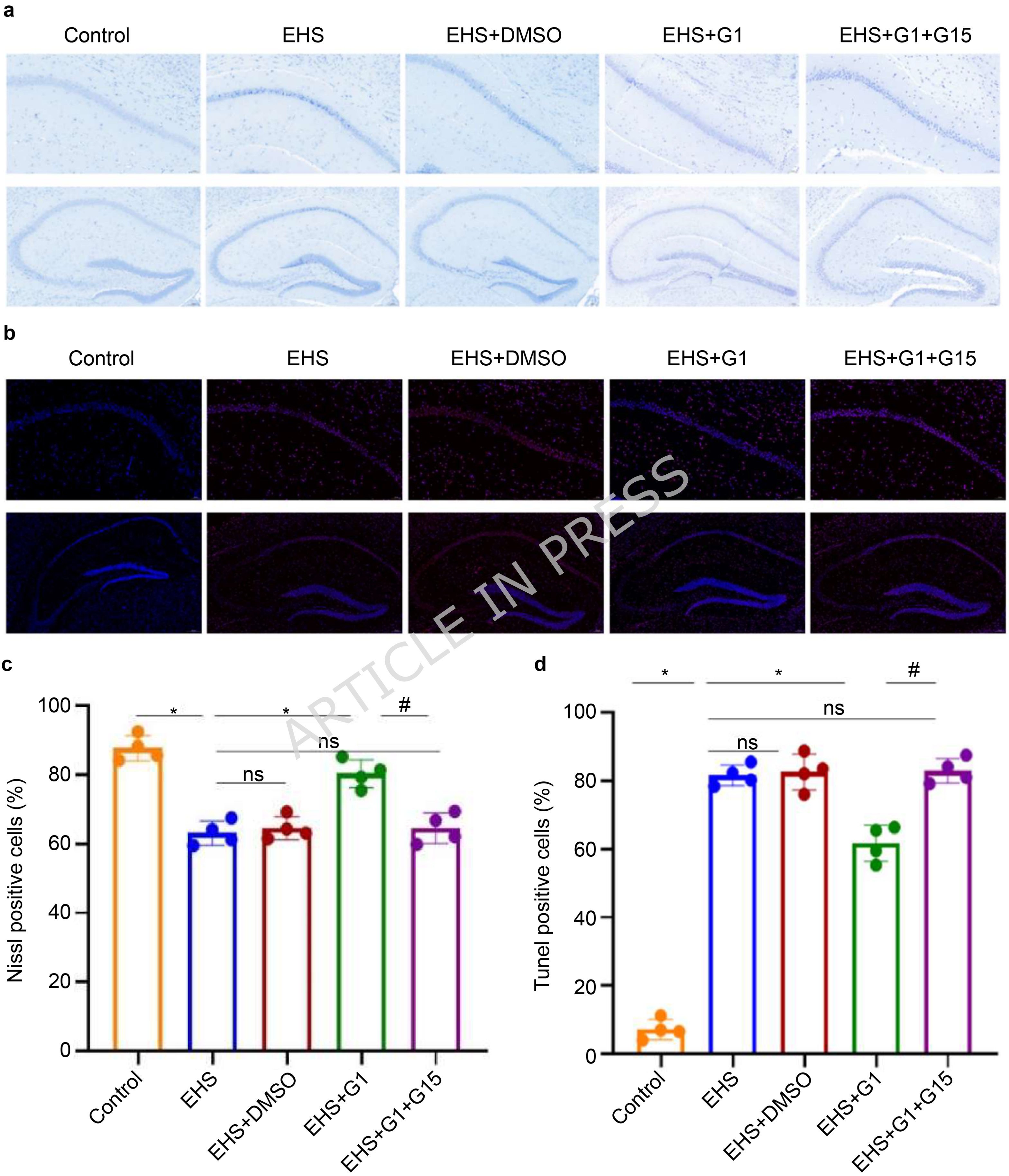
a
Control
EHS
EHS+DMSO
EHS+G1
EHS+G1+G15
b
Control
EHS
EHS+DMSO
EHS+G1
EHS+G1+G15
c
Nissl positive cells (%)
100
80
60
40
20
0
*
*
#
ns
ns
Control
EHS
EHS+DMSO
EHS+G1
EHS+G1+G15
d
Tunel positive cells (%)
100
80
60
40
20
0
*
*
#
ns
ns
Control
EHS
EHS+DMSO
EHS+G1
EHS+G1+G15

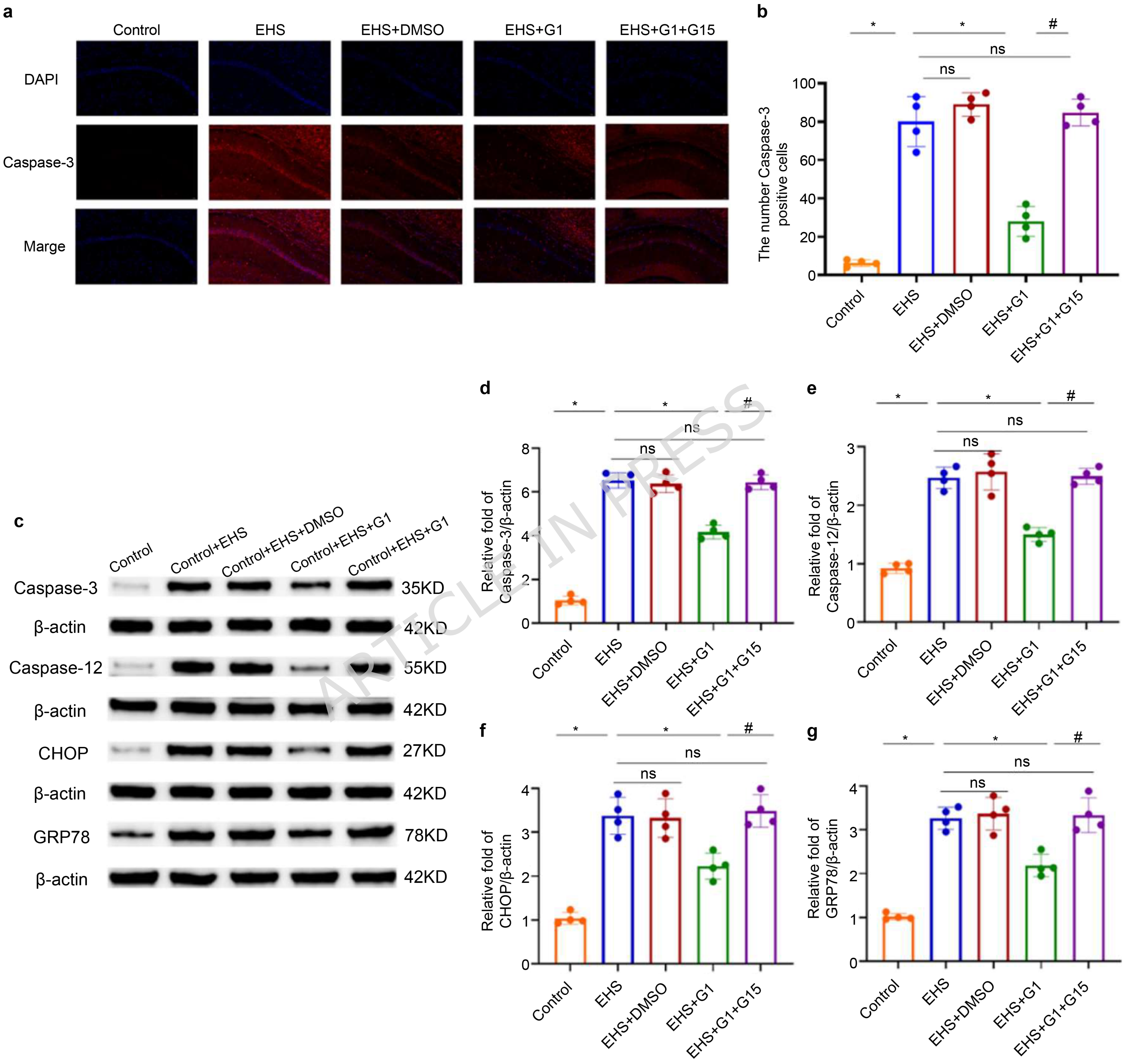
a
Control
EHS
EHS+DMSO
EHS+G1
EHS+G1+G15
DAPI
Caspase-3
Marge
b
The number Caspase-3 positive cells
0
20
40
60
80
100
*
*
#
ns
ns
Control
EHS
EHS+DMSO
EHS+G1
EHS+G1+G15
c
Control
Control+EHS
Control+EHS+DMSO
Control+EHS+G1
Control+EHS+G1
Caspase-3
35KD
β-actin
42KD
Caspase-12
55KD
β-actin
42KD
CHOP
27KD
β-actin
42KD
GRP78
78KD
β-actin
42KD
d
Relative fold of Caspase-3/β-actin
0
2
4
6
8
*
*
#
ns
ns
Control
EHS
EHS+DMSO
EHS+G1
EHS+G1+G15
e
Relative fold of Caspase-12/β-actin
0
1
2
3
*
*
#
ns
ns
Control
EHS
EHS+DMSO
EHS+G1
EHS+G1+G15
f
Relative fold of CHOP/β-actin
0
1
2
3
4
*
*
#
ns
ns
Control
EHS
EHS+DMSO
EHS+G1
EHS+G1+G15
g
Relative fold of GRP78/β-actin
0
1
2
3
4
*
*
#
ns
ns
Control
EHS
EHS+DMSO
EHS+G1
EHS+G1+G15